LETTERS

The development of a protoplanetary disk from its natal envelope

Dan M. Watson[1], C. J. Bohac[1], C. Hull[1,2], William J. Forrest[1], E. Furlan[3,4], J. Najita[5], Nuria Calvet[6], Paola d'Alessio[7], Lee Hartmann[6], B. Sargent[1], Joel D. Green[1], Kyoung Hee Kim[1] & J. R. Houck[8]

Class 0 protostars, the youngest type of young stellar objects, show many signs of rapid development from their initial, spheroidal configurations, and therefore are studied intensively for details of the formation of protoplanetary disks within protostellar envelopes. At millimetre wavelengths, kinematic signatures of collapse have been observed in several such protostars, through observations of molecular lines that probe their outer envelopes. It has been suggested that one or more components of the proto-multiple system NGC 1333–IRAS 4 (refs 1, 2) may display signs of an embedded region that is warmer and denser than the bulk of the envelope[3,4]. Here we report observations that reveal details of the core on Solar System dimensions. We detect in NGC 1333–IRAS 4B a rich emission spectrum of H_2O, at wavelengths 20–37 μm, which indicates an origin in extremely dense, warm gas. We can model the emission as infall from a protostellar envelope onto the surface of a deeply embedded, dense disk, and therefore see the development of a protoplanetary disk. This is the only example of mid-infrared water emission from a sample of 30 class 0 objects, perhaps arising from a favourable orientation; alternatively, this may be an early and short-lived stage in the evolution of a protoplanetary disk.

NGC 1333–IRAS 4B (henceforth IRAS 4B) and its neighbour NGC 1333–IRAS 4A (IRAS 4A) lie about 320 pc away[5]. Considered among the archetypal protostars, they are often taken to be a proto-triple system, with IRAS 4B single, and IRAS 4A a 1.8-arcsec binary (projected separation 600 AU), 31 arcsec away from IRAS 4B (ref. 6). Both IRAS 4A and IRAS 4B have high-velocity outflows[7,8]. That of IRAS 4B is not well resolved spatially, but is presumed to be bipolar, viewed close to the outflow axis[1,2]. Both also have dense, cold, approximately spheroidal envelopes, which are resolved at millimetre and submillimetre wavelengths. Millimetre-wavelength tracers of dense molecular gas reveal kinematic symptoms of collapse in both envelopes[1,2]. IRAS 4A is marginally detected in Spitzer Space Telescope-Infrared Array Camera (IRAC) images, and IRAS 4B not at all; only extended emission, resembling scattered light from an outflow cavity viewed close to its axis, is seen by IRAC at 3.6 μm and 4.5 μm (R. A. Gutermuth, personal communication).

A decade ago, the ISO Long-wavelength Spectrograph (ISO-LWS) was used to observe the IRAS 4 system[3,4]. With its 90-arcsec beam, this instrument could not resolve IRAS 4A from IRAS 4B, but it did detect many emission lines thereabouts, among them several low-lying rotational transitions of H_2O. Under the assumption that the water emission arises equally from IRAS 4A and IRAS 4B, observers[3] showed that this emission probably probes a cold outer component of the envelopes, and an inner component warm enough ($T > 120$ K) that dust-grain mantles have sublimated to increase greatly the gas-phase abundance of water. They could not, however, rule out an origin of the water emission in the outflows associated with IRAS 4A and IRAS 4B.

IRAS 4A and IRAS 4B are part of a sample of 30 class 0 objects, which we observed with the Spitzer Infrared Spectrograph (IRS) in 2004–5. Initially we observed these objects in low spectral resolution ($\lambda/\Delta\lambda = 60$–120), with results as shown in Fig. 1. In many of the surveyed objects we detect spectral lines of molecular hydrogen, and fine-structure lines of low-ionization-potential ions and atoms, usually associated with outflows. One line of this type—[S I] at 25.249 μm—is the only emission feature that appears in the 20–40-μm wavelength range for IRAS 4A. The spectrum of IRAS 4B, however, is unique in our sample: it contains many emission features suggestive of spectrally unresolved H_2O lines with a wide range of excitation. We re-observed IRAS 4B in March 2006 with the high-resolution ($\lambda/\Delta\lambda = 600$) IRS module, and confirmed this suggestion

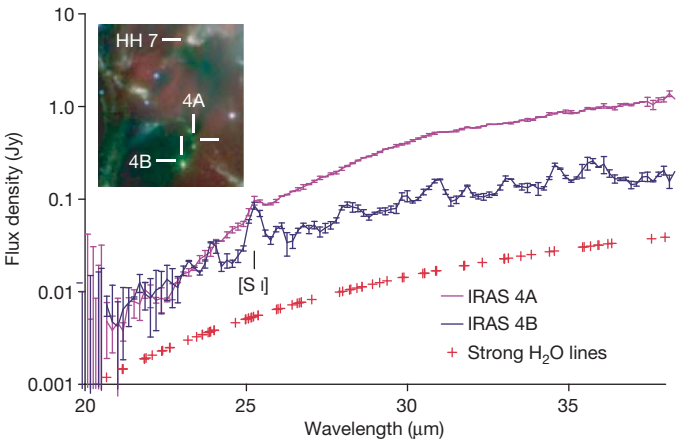

Figure 1 | Spitzer-IRS low-resolution spectra of IRAS 4A and IRAS 4B, and false-colour mid-infrared image. Main panel, spectra of IRAS 4A (magenta trace) and IRAS 4B (blue trace); error bars represent the standard deviations of the flux values in each spectral channel. Wavelengths of strong lines of water, which give rise to blended emission features in the low-resolution spectrum of IRAS 4B, are indicated with red crosses. The IRAS 4 system has total luminosity $28L_\odot$ (ref. 19); from these spectra it appears that $4.2L_\odot$ belongs to IRAS 4B, and the rest to the two components of IRAS 4A. See Supplementary Information for data-reduction details. Inset, part of the Spitzer-IRAC image-set for NGC 1333 (R. A. Gutermuth, personal communication), with 3.6 μm shown in blue, 4.6 μm in green and 8 μm in red, and positions indicated for IRAS 4A and IRAS 4B, and for the nearby HH 7.

[1]Department of Physics and Astronomy, University of Rochester, Rochester, New York 14627-0171, USA. [2]Department of Astronomy, University of Virginia, Charlottesville, Virginia 22904, USA. [3]NASA Astrobiology Institute, and [4]Department of Physics and Astronomy, UCLA, Los Angeles, California 90095, USA. [5]NOAO, Tucson, Arizona 85719, USA. [6]Department of Astronomy, University of Michigan, Ann Arbor, Michigan 48109, USA. [7]Centro de Radioastronomía y Astrofísica, UNAM, 58089 Morelia, Michoacán, Mexico. [8]Center for Radiophysics and Space Research, Cornell University, Ithaca, New York 14853, USA.

in detail (Fig. 2). Besides the [S I] 25.249 μm and [Si II] 34.815 μm lines, which can be ascribed to IRAS 4B's outflow, we detect a total of 48 spectral lines that we can assign to 75 pure-rotational transitions of H_2O, seen either singly or in spectrally unresolved combinations. Significantly, all of these lines belong to the ground vibrational manifold of $H_2{}^{16}O$; no vibrationally excited or 'isotopic' water lines are seen. Only the lines at wavelengths greater than 29.8 μm have ever been detected outside the Solar System before, and those only in bright supergiant stars[9,10]. We also detect seven narrow emission features that we have not succeeded in identifying, but that cannot be due to any well-known molecular or atomic transitions. In the following we will discuss the water-line emission exclusively.

Many important features of the physical state of the emitting material are obtained to good approximation from a simple, conventional model: a plane-parallel slab, with uniform temperature, density high enough that the rotational energy levels of water have thermal-equilibrium populations, and velocity gradient large compared with the ratio of thermal speed and slab thickness. Radiative transfer is included via the escape-probability formalism[4,11]. We leave the slab's temperature, water column density and emitting area, the extinction towards the slab, and the background continuum temperature, as free parameters. Figure 2 is a plot of the observed spectrum and best-fitting model, and Table 1 a list of model parameters and other quantities we derive from the observations.

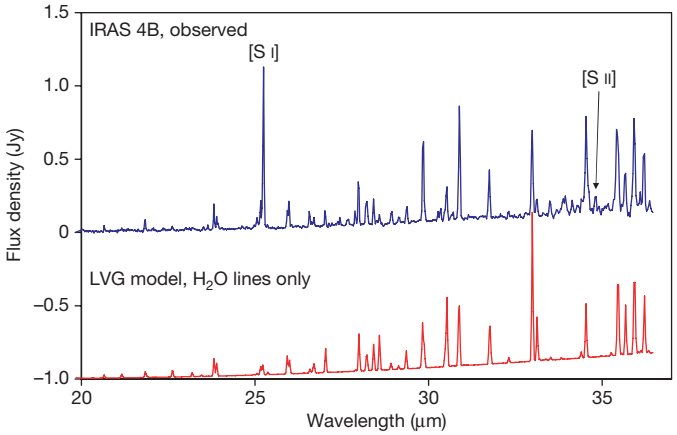

Figure 2 | Comparison of observed and model spectra of IRAS 4B. With the exceptions of the lines of [S I] and [S II] labelled in the plot, the emission lines in the observed spectrum (top) are due to ground-vibrational-state, rotational transitions of $H_2{}^{16}O$. (See Supplementary Information for data-reduction and line-identification details.) The model spectrum (bottom) is offset by −1.0 Jy. It is based on a plane-parallel slab, with uniform temperature and density and a large velocity gradient (LVG), treated with the escape-probability formalism[4,11]. Outside the slab we assume interstellar-like extinction[20] from a foreground screen. Parameters of water (energy levels, *A*-coefficients, and so on) we adopt from the HITRAN database[21]. We suppose that the rotational levels are excited by collisions with hydrogen molecules, and neglect radiative pumping. The latter assumption is justified after modelling, as the line opacities and background intensity are small. However, accurate collisional excitation rate coefficients are only available for two-thirds of the states involved[22,23]. As a first approximation, we assume thermal-equilibrium populations, and an *ortho*/*para* abundance ratio of 3. The assumption of thermal equilibrium implies a molecular hydrogen density approaching these states' critical densities for collisional de-excitation, which lie in the range 10^{10}–10^{12} cm^{-3} (see Supplementary Information). The results are not sensitive to the isotopologue relative abundances, for which we adopt the solar abundances of oxygen and hydrogen isotopes. The continuum beneath the lines is blackbody emission to high accuracy, which presumably arises from the optically thick disk behind, or at larger radii than, the slab. This leaves slab temperature, water column density, emitting area, extinction and continuum temperature as free parameters, and we have varied these parameters to produce a minimum-χ^2 fit, with reduced $\chi^2 = 16$ (see Table 1).

Table 1 | Model parameters and inferred quantities for the core of IRAS 4B

Disk-surface density	Thermal equilibrium, requiring molecular hydrogen density of at least 10^{10} cm^{-3}
Disk-surface temperature	170 K
Extinction by envelope	$A_V = 100$ mag, interstellar-like
H_2O column density	9.2×10^{16} cm^{-2} (each face of disk)
H_2O-line-emitting mass	7.5×10^{24} g (H_2O), $\sim 6 \times 10^{27}$ g (total)
Emitting area	6,000 AU^2 (each face of disk)
Accretion shock speed	2 km s^{-1}
Total H_2O-line luminosity	$0.03 L_\odot$ (extinction-corrected)
Disk accretion rate	$\geq 0.7 \times 10^{-4}\, M_\odot$ yr^{-1} (total)
Continuum temperature (underlying disk and envelope)	59 K

Except for the density, these values result from the model fit to the observed spectrum in Fig. 2. Formally, the temperatures are uncertain by ±2 K, and the extinction is uncertain by ±50 mag in A_V. The uncertainties in the remaining quantities are dominated by that in the extinction (see Supplementary Information), and are not independent of one another; typically, the maximum uncertainty in these quantities is approximately a factor of two.

The good model fit demonstrates that all the observed rotational states of water are indeed populated close to thermal equilibrium, so the molecular-hydrogen density must approach or exceed these states' critical densities for collisional de-excitation, 10^{10}–10^{12} cm^{-3}. This is many orders of magnitude too dense to be associated with IRAS 4B's outflow or outer envelope: the source of emission must be in the vicinity of the protostar. But it is not particularly hot at the core of IRAS 4B. The highest-excitation lines we observe are very temperature-sensitive; their faintness relative to the others indicates that there is little material warmer than 170 K.

Predictions from spherical collapsing-envelope models of class 0 objects[12,13] do not match the observed spectrum; nor do the combinations of density, temperature and emitting area in these models resemble those we have inferred. Our model values are, however, appropriate for dense gaseous disks embedded within such envelopes[14,15]. Thus the water emission probably shows us, we believe for the first time, accretion from a protostellar envelope by a protoplanetary disk[14–16]. In Fig. 3 we sketch a cross-section of this arrangement of collapsing envelope and disk. Radiation heating would not suffice to heat such a large area of the disk to 170 K (ref. 17), nor would shocks from spiral density waves; an accretion shock is probably involved. Complex models of our spectrum of IRAS 4B should thus reveal many long-sought details of the assembly of protoplanetary disks.

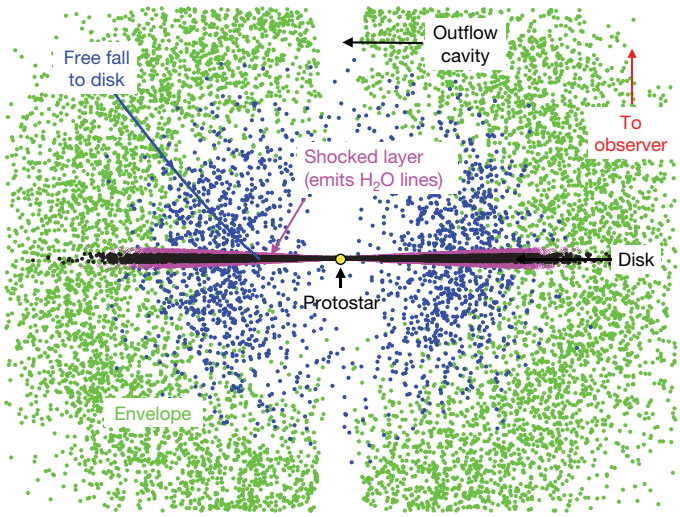

Figure 3 | Cartoon depiction of our model for IRAS 4B. One example streamline (blue line with arrows, top left) is shown to illustrate the infall from the rotating envelope onto the disk[14]. The molecular-hydrogen density of the infalling gas (green dots, blue dots) reaches roughly 3×10^9 cm^{-3} or greater (see Supplementary Information) before encountering the disk (black). There the material's deceleration in a 2 km s^{-1} accretion shock produces the warm, extremely dense ($>10^{10}$ cm^{-3}) layer (magenta), with properties as in Table 1, that in turn produces the water-line emission we detect. Our view of the object, as indicated, is close to face-on.

According to the model, the brightest lines have peak optical depth $\tau = 6$–10, but most of the others are optically thin. From the gas temperature and flux of the optically thick lines, we calculate the emitting area to be 6,000 AU^2 on the side facing us. From the optically thin lines we obtain the mass of water, 7.5×10^{24} g, counting both disk faces. Assuming that all of the solar abundance of oxygen not taken up by CO is present in the gas phase as water ($H_2O/H_2 = 1.5 \times 10^{-4}$)—consistent with rapid sublimation of dust-grain ice mantles expected at $T = 170$ K—the total gas mass is $\sim 6 \times 10^{27}$ g ($\sim M_{\rm Earth}$). The detected water, if condensed, would fill the Earth's oceans about five times.

Also according to the model, the detected water emission comprises about 30% of the total luminosity emitted from water. (The model also predicts far-infrared water lines fainter than those detected by ISO-LWS[3,4], suggesting that the latter observations were dominated either by the envelope or the outflow.) Corrected for extinction and this fraction, the water-line luminosity radiated by both faces of the disk is $0.03 L_\odot$ (where $L_\odot$ is the solar luminosity). Usually[15,18], water emission is the dominant coolant of dense molecular material.

Consider material in the envelope, falling freely from a great distance at a steady rate $\dot{m}$ to the disk at radius r, and entering a single, non-magnetic shock at speed v. The post-shock gas temperature T and cooling luminosity L are given by

$$L = \frac{1}{2}\dot{m}v^2 = \frac{GM\dot{m}}{r} \quad , \qquad T = \frac{2(\gamma-1)}{(\gamma+1)^2}\frac{\mu}{k}v^2 \quad , \tag{1}$$

where M is the mass of the protostar, μ the mean molecular mass ($\sim m(H_2)$), γ the ratio of specific heats ($\sim 7/5$), G the gravitational constant, and k Boltzmann's constant. We have measured T and L, and thence obtain $v = 2\,{\rm km\,s^{-1}}$ and $\dot{m} = 0.7 \times 10^{-4} M_\odot {\rm yr}^{-1}$ (where $M_\odot$ is the solar mass) similar to that inferred for the outer envelope's infall rate[1,2], and much greater than would be inferred for the protostar from its luminosity. We can also evaluate combinations of M and r; for example, if $r = 50$ AU, then $M = 0.14 M_\odot$, and the shock extends over a $r = 40$–60 AU annulus.

At such high density (10^{10}–10^{11} cm^{-3}), heating of dust in gas-grain collisions, along with optically thin thermal radiation by this dust, is probably a significant coolant of the post-shock gas. Accordingly, we should regard the mass accretion rate obtained above as a lower limit to the actual rate.

IRAS 4B is alone in our sample of class 0 objects in its mid-infrared water-line emission, and the inferred disk-accretion activity. Perhaps high extinction and unfavourable line-of-sight orientation obscure such emission in the other systems. Alternatively—and more interestingly—we may have observed an early and short-lived stage of protoplanetary disk formation.

Received 2 August 2006; accepted 2 July 2007.

1. Choi, M., Panis, J.-F. & Evans, N. J. II Berkeley-Illinois-Maryland Association Survey of protostellar collapse candidates in HCO^+ and HCN lines. *Astrophys. J. Suppl.* **122,** 519–556 (1999).
2. Di Francesco, J., Myers, P. C., Wilner, D. J., Ohashi, N. & Mardones, D. Infall, outflow, rotation, and turbulent motions of dense gas within NGC 1333 IRAS 4. *Astrophys. J.* **562,** 770–789 (2001).
3. Maret, S., Ceccarelli, C., Caux, E., Tielens, A. G. G. M. & Castets, A. Water emission in NGC 1333 – IRAS 4. *Astron. Astrophys.* **395,** 573–585 (2002).
4. Ceccarelli, C. *et al.* Water line emission in low-mass protostars. *Astron. Astrophys.* **342,** L21–L24 (1999).
5. de Zeeuw, P. T., Hoogerwerf, R., de Bruijne, J. H. J., Brown, A. G. A. & Blaauw, A. A. HIPPARCOS census of the nearby OB associations. *Astron. J.* **117,** 354–399 (1999).
6. Looney, L. W., Mundy, L. G. & Welch, W. J. Unveiling the circumstellar envelope and disk: a subarcsecond survey of circumstellar structures. *Astrophys. J.* **529,** 477–498 (2000).
7. Knee, L. B. G. & Sandell, G. The molecular outflows in NGC 1333. *Astron. Astrophys.* **361,** 671–684 (2000).
8. Blake, G. A. *et al.* A molecular line study of NGC 1333/IRAS 4. *Astrophys. J.* **441,** 689–701 (1995).
9. Neufeld, D. A., Feuchtgruber, H., Harwit, M. & Melnick, G. J. Infrared Space Observatory observations of far-infrared rotational emission lines of water vapour toward the supergiant star VY Canis Majoris. *Astrophys. J.* **517,** L147–L150 (1999).
10. Neufeld, D. A. *et al.* Detection of far-infrared rotational lines of water vapour toward W Hydrae. *Astron. Astrophys.* **315,** L237–L240 (1996).
11. Scoville, N. Z. & Solomon, P. M. Radiative transfer, excitation, and cooling of molecular emission lines. *Astrophys. J.* **187,** L67–L71 (1974).
12. Ceccarelli, C., Hollenbach, D. J. & Tielens, A. G. G. M. Far-infrared line emission from collapsing protostellar envelopes. *Astrophys. J.* **471,** 400–426 (1996).
13. Doty, S. D. & Neufeld, D. A. Models for dense molecular cloud cores. *Astrophys. J.* **489,** 122–142 (1997).
14. Cassen, P. & Moosman, A. On the formation of protostellar disks. *Icarus* **48,** 353–376 (1981).
15. Neufeld, D. A. & Hollenbach, D. J. Dense molecular shocks and accretion onto protostellar disks. *Astrophys. J.* **428,** 170–185 (1994).
16. Ulrich, R. K. An infall model for the T Tauri phenomenon. *Astrophys. J.* **210,** 377–391 (1976).
17. Kenyon, S. J., Calvet, N. & Hartmann, L. The embedded young stars in the Taurus-Auriga molecular cloud. I — Models for spectral energy distributions. *Astrophys. J.* **414,** 676–694 (1993).
18. Neufeld, D. A. & Kaufman, M. J. Radiative cooling of warm molecular gas. *Astrophys. J.* **418,** 263–272 (1993).
19. Sandell, G., Aspin, C., Duncan, W. D., Russell, A. P. G. & Robson, E. I. NGC 1333 IRAS 4: a very young, low-luminosity binary system. *Astrophys. J.* **376,** L17–L20 (1991).
20. Weingartner, J. C. & Draine, B. T. Dust grain-size distributions and extinction in the Milky Way, Large Magellanic Cloud, and Small Magellanic Cloud. *Astrophys. J.* **548,** 296–309 (2001).
21. Rothman, L. S. *et al.* The HITRAN 2004 molecular spectroscopic database. *J. Quant. Spectrosc. Radiat. Transf.* **96,** 139–204 (2004).
22. Green, S., Maluendes, S. & McLean, A. D. Improved collisional excitation rates for interstellar water. *Astrophys. J. Suppl.* **85,** 181–185 (1993).
23. Phillips, T. R., Maluendes, S. & Green, S. Collisional excitation of H_2O by H_2 molecules. *Astrophys. J.* **107,** 467–474 (1996).

Supplementary Information is linked to the online version of the paper at www.nature.com/nature.

Acknowledgements This work was supported in part by NASA through the Spitzer-IRS Instrument Team, Origins and Astrobiology programmes, and by CONACyT (México). We are grateful to R. Gutermuth for use of the Spitzer-IRAC data on NGC 1333, and to M. Jura, L. Keller, G. Sloan and D. Hollenbach for discussions.

Author Information Reprints and permissions information is available at www.nature.com/reprints. The authors declare no competing financial interests. Correspondence and requests for materials should be addressed to D.M.W. (dmw@pas.rochester.edu).